Journal of Inflammation Research

Dovepress
open access to scientific and medical research

Open Access Full Text Article

ORIGINAL RESEARCH

Xianglian Zhixie Tablet Antagonizes Dextran Sulfate Sodium-Induced Ulcerative Colitis by Attenuating Systemic Inflammation and Modulating Gut Microbiota

Yilin Li[1,*], Tingting Wang[2,*], Beibei Ma[2], Shangyue Yu[1], Hailuan Pei[1], Shiqiu Tian[1], Yingying Tian[1], Chuang Liu[1], Xinyue Zhao[1], Zeping Zuo[2], Zhibin Wang[1,2]

[1]School of Chinese Pharmacy, Beijing University of Chinese Medicine, Beijing, People's Republic of China; [2]Beijing Tongrentang Technology Co., LTD. Pharmaceutical Factory, Beijing, People's Republic of China

*These authors contributed equally to this work

Correspondence: Zhibin Wang; Zeping Zuo, Beijing Tongrentang Technology Co., LTD. Pharmaceutical Factory, No. 20S 3rd Ring Road Middle, Beijing, 100071, People's Republic of China, Email wangzhibin4804@126.com; zepingzuo@126.com

Purpose: Xianglian Zhixie Tablet (XLZXT), a classical traditional Chinese medicine formulation, is commonly used to treat Ulcerative Colitis (UC) in China. However, the therapeutic mechanisms of XLZXT for UC have yet to be fully understood. This study aimed to investigate the curative benefits of XLZXT and its associated mechanisms for healing UC in mice.

Methods: In the present study, the 1% dextran sulfate sodium (DSS) solution was used to establish the UC model in C57BL/6N mice. To investigate the therapeutic effects of XLZXT on DSS-induced UC mice, several parameters were measured, including DAI score, colon length, spleen index, pathological changes in colon tissue, and levels of inflammatory factors in plasma and colon tissue. By investigating the gut microbiota, assessing the levels of intestinal mucosal protein expression, and looking at the proteins involved in the TLR4/MyD88/NF-B p65 signaling pathway, the mechanisms of XLZXT impact on UC were investigated. Mouse feces were examined for patterns of gut microbiota expression using high-throughput sequencing of 16S rRNA.

Results: XLZXT effectively alleviated UC symptoms and colon pathological damage in DSS-induced UC mice. It improved body weight loss, stool consistency, and hematochezia, while also repairing colon damage. Moreover, it down-regulated pro-inflammatory cytokines (such as TNF-α, IL-1β, and IL-6), and up-regulated anti-inflammatory cytokines (such as IL-10). XLZXT also increased the expression of MUC-2, Occludin and ZO-1, while decreasing the expression of NF-κB, MyD88 and TLR4. Additionally, it regulated gut microbiota disorder by increasing the abundance of beneficial bacteria and reducing the adhesion of intestinal harmful bacteria.

Conclusion: XLZXT demonstrated therapeutic effects on DSS-induced UC mice. The mechanisms may be associated with repairing the intestinal mucosal barrier, regulating the TLR4/MyD88/NF-κB p65 signaling pathway, and restoring the balance of gut microbiota.

Plain Language Summary: This is the first study to probe the therapeutic potential of XLZXT for UC. Our findings indicated that XLZXT could effectively alleviate the clinical symptoms of UC and in-depth apparently modify the levels of relevant cytokines in the organism to maintain the system homeostasis. Our results suggested that XLZXT might treat DSS-induced UC by repairing the intestinal mucosa barrier, regulating the TLR4/MyD88/NF-κB p65 signaling pathway, and restoring gut microbiota balance.

Keywords: ulcerative colitis, TCM, TLR4/MyD88/NF-κB p65 signaling pathway, gut microbiota

Introduction

Ulcerative colitis (UC) is a chronic inflammatory disease of the intestines that has an unclear etiology and pathogenesis. It is one of two primary forms of inflammatory bowel disease (IBD).[1] UC is characterized by diffuse inflammation and ulcerative

Received: 20 June 2023
Accepted: 20 September 2023
Published: 28 September 2023

Graphical Abstract

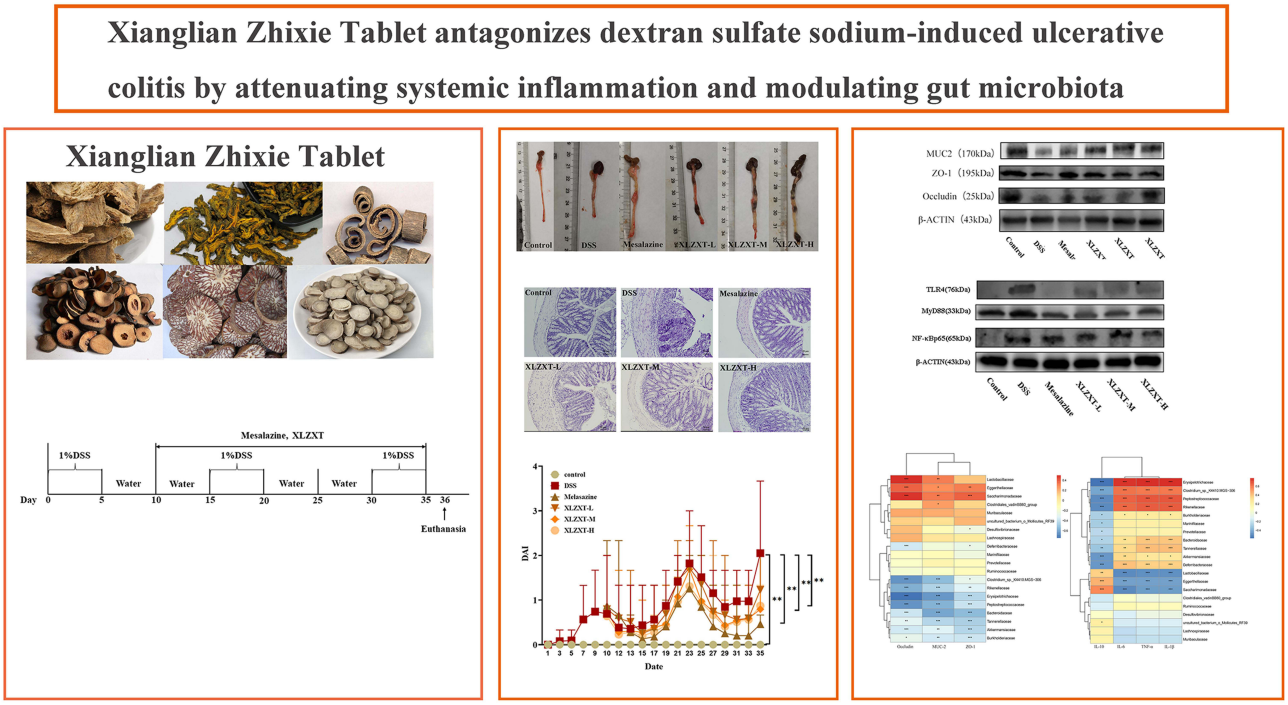

lesions in the rectum, colon mucosa, and submucosa. It is a long-lasting disease that is difficult to cure, often recurring and prone to carcinogenesis.[2,3] Patients usually experience recurrent episodes of mucous bloody stool, diarrhea, tenesmus, urgent defecation, and abdominal pain.[4] Most scholars believe that the pathogenesis of UC is largely related to genetics, environment, infection, immunity, and mental psychology. The primary symptoms of UC are increased intestinal mucosal permeability caused by intestinal inflammation, reduced intestinal mucosal barrier function, and intestinal mucosal necrosis.[2,5,6] Currently, the primary objectives in treating UC patients are centered on reducing the inflammatory response, promoting the repair of the intestinal mucosa, and enhancing the function of the intestinal mucosal barrier.[7,8] Prolonged administration of high doses of conventional Western medicine therapeutic drugs may cause several negative effects, including nausea, headaches, anemia, stomach burning, and reversible male infertility.[9,10] On the one hand, the new biological agents are costly; on the other hand, the fecal microbiota transplantation method demands a certain degree of psychological resilience from the patient.[11] Consequently, it is crucial to explore the availability of effective drugs with minimal adverse reactions.

The original prescription of Xianglian Zhixie Tablet (XLZXT) is derived from "Xianglian Huazhi Pill" with flavor reduction in Shen's Work on the Importance of Life Preservation written by Shen Jinao of Qing Dynasty, which is made up of six Chinese herbs, namely Aucklandia lappa (Muxiang, Aucklandia lappa Decne.), Coptis chinensis (Huanglian, Coptis chinensis Franch.), Magnolia officinalis (Houpo, Magnolia officinalis Rehd.et Wils.), Citrus aurantium (Zhishi, Citrus aurantium L.), Areca catechu (Binlang, Citrus aurantium L.) and Paeonia lactiflora Pall. (Baishao, Paeonia lactiflora Pall.), the six herbs are prepared in equal proportions into XLZXT. Although the term "ulcerative colitis" is not used in Traditional Chinese Medicine (TCM), contemporary physicians have classified it as many types of TCM terms, including "dysentery", "diarrhea", "blood in stool" and "intestinal wind" based on clinical manifestations such as mucus and blood in the stool, stomach pain, diarrhea, and shortness of breath.[12] According to the Ministry of Health of the People's Republic of China drug standards - Chinese medicine prescription preparations (WS3-B-1785-94, Z9-128), XLZXT is primarily used to clear heat and dampness, and stagnation of dysentery. The medicine is indicated to treat symptoms such as red and white dysentery caused by heat in the intestines, abdominal pain and drops, tasteless diet, and

tiredness of the limbs, which are considered to be associated with large intestine damp-heat UC in TCM. Studies have shown that XLZXT is useful in treating UC patients.[13–15] XLZXT was specifically included as a therapy for UC with large intestine damp-heat syndrome in the 2011 publication of Guidelines for the Diagnosis and therapy of UC. However, XLZXT's mode of action has not yet been investigated. In order to offer theoretical evidence for the clinical use of XLZXT against UC, the therapeutic effects and mechanisms of XLZXT on UC mice were examined in this work.

Materials and Methods

Animals

Male C57BL/6N mice with a specific pathogen-free status were acquired from Beijing Vital River Laboratory Animal Technology Co. Ltd. (Beijing, China). The mice weigh 20–24 g and are around 8 weeks old. All animals were free access to food and water during the trial. Additionally, each mouse was housed in an animal room with a 12-hour cycle of darkness and light at a temperature of 21±2 °C and a humidity of 55±5%. All experimental procedures were conducted in accordance with "Guidelines for the Management and Use of Laboratory Animals" (Ministry of Science and Technology, China, 2006), and the study was approved by Experimental Animal Ethics Committee of the Research Institute of Beijing Tongrentang Co. LTD with the ethical approval number YJY-2021-030904.

Reagents

Mesalazine sustained-release particles (Shanghai Ethypharm Pharmaceuticals Co., Ltd. batch number 200906). DSS (MP Biomedicals). Enzyme-linked immunosorbent assay kits and the total protein assay kit (with standard BCA method) were obtained from Nanjing Jiancheng Bioengineering Institute (Jiangsu, China). MUC-2 anti-body, Occludin anti-body, ZO-1 anti-body, TLR4 anti-body, and MyD88 anti-body were purchased from Abcam (Shanghai, China). NF-κB p65 anti-body was purchased from Cell Signaling Technology (Boston, USA); TGuide S96 Magnetic Soil /Stool DNA Kit (Tiangen Biotech (Beijing) Co., Ltd.); Omega DNA purification kit (Omega Inc., Norcross, GA, USA).

Preparation of XLZXT Sample

Xianglian Zhixie Tablets were provided by Beijing Tongrentang Technology Co., LTD. Pharmaceutical Factory (Lot: 20120387). The preparation method of Xianglian antidiarrheal tablets is as follows: Coptis chinensis and Paeonia lactiflora Pall were crushed into fine powder; Areca catechu with water decoction twice, filtered, combined filtrate; Magnolia officinalis with 70% ethanol heating reflux extraction two times, filtration, combined filtrate, recovery of ethanol to no alcohol flavor; the volatile oil was extracted from Aucklandia lappa and Citrus aurantium. The distilled water solution was combined with the above two kinds of filtrates, and the paste with a relative density of 1.35~1.40 (50 °C) was concentrated under reduced pressure. The paste was mixed with the above powder, dried, crushed into fine powder, granulated with dilute ethanol, dried, added with Radix Aucklandiae and Fructus Aurantii Immaturus volatile oil, mixed, pressed into 1000 pieces. After grinding, Xianglian Zhixie tablets were prepared into 67.82 mg/mL, 135.63 mg/mL, 271.62 mg/mL suspension with ultrapure water for intragastric administration in mice.

Animal Model Establishment and Treatment Procedures

84 C57BL/6N mice were separated randomly into the blank group (n=13) and the model group (n=71) after one week of adaptive feeding. The fresh DSS solution was prepared every two days. In the control group, the mice drank sterile water. As shown in Figure 1, mice in the model group were given 1%DSS and sterile water alternately. On the ninth day of the experiment, one mouse from the blank group and six mice from the model group were randomly selected for killing, and the colon was taken to check whether the UC mouse model had been successfully replicated based on DAI scores and histopathology. Sixty-five mice with successful modeling were randomly divided into the model group (n=13), mesalazine group (310 mg/kg, n=13), XLZXT low-dose group (678.2 mg/kg, n=13), XLZXT tablet middle-dose group (1356.3 mg/kg, equivalent to human clinical equivalent dose, n=13) and XLZXT high-dose group (2716.2 mg/kg, n=13) according to body weight. Once a day starting on the tenth day until the end of the experimental cycle, the mice were administrated with a dose

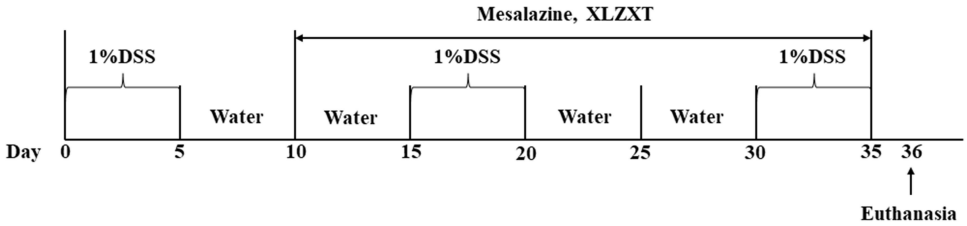

Figure 1 All procedures for model establishment and drug administration.

volume of 0.2 mL/10 g by gavage once a day (ie, 26 days of administration). Mice in the control group (n=12) and the model group were given the same amount of sterile water. The total experimental period was 35 days.

On 36th day, 1% pentobarbital sodium was administered intraperitoneally (0.1 mL/10 g) to anesthetize all the animals. Blood was collected from the abdominal main vein (EDTA anticoagulant). Plasma was separated after being centrifuged at 3000 rpm/min for 10 min at −4 °C and stored at −80 °C. The spleen was weighed and stored in a refrigerator at −80 °C. The spleen index was calculated according to the formula: Spleen index=Spleen mass/body mass. Following colon length measurement, 0.5 cm was fixed in 4% paraformaldehyde, and the remaining material was kept in a freezer at −80 °C for future research.

The Disease Activity Index (DAI) Score

Every two days during the modeling period, the mice's body weight was recorded, together with the stool condition, the level of hematochezia, and the DAI score. The weight loss score, stool pattern score, and hematochezia score were averaged to create the DAI score. After administration, DAI was scored every two days to analyze the effect of modeling and administration. Table 1 lists the scoring standards.[16]

Histopathology Evaluation

Colon segments were fixed in a 4% paraformaldehyde standing solution for at least 24 h. They were prepared as wax blocks and then segmented to a thickness of 4 μm. The sections were stained with HE or PAS and observed under a microscope at ×200 magnifications. Observed pathological damage of the colon and calculated colon mucosa damage index (CMDI) score. The CMDI score was the average of scores of colonic ulcer, interstitial edema and neutrophil infiltration. The criteria for pathology scores are listed in Table 2. The sections stained with PAS were used to observe changes in morphology, number and secretion of goblet cells. Referring to the goblet cell counting method, the number of goblet cells stained by PAS was computed and evaluated.

Elisa Assay

The colon tissues were homogenized in ice-cold PBS (pH 7.4) and then centrifuged for 20 minutes at 3500 rpm at 4 °C to separate the supernatants to get the colon homogenate. Following the directions on the ELISA kits, the levels of IL-6,

Table 1 Scoring System for Calculating the DAI

Score	Weight Loss (%)	Stool Consistency	Blood
0	0	Normal	None
1	1–5	Soft but still formed	Positive occult blood
2	5–10	Soft	Visible mild blood stools
3	10–15	Very soft; wet	Visible blood stools
4	> 15	Watery diarrhea	Blood fills the colon

Table 2 Scoring System for Calculating the CMDI

Score	Ulceration	Interstitial Edema	Neutrophil Immersion
0	None	None	None
1	Erosions or single ulcers	Mild	<10/HPF
2	1–3 ulcers	Moderate	10–50/HPF
3	>3 ulcers	Severe	>50/HP

Notes: HPF (High Power Field) generally refers to the field of view of pathological sections that can be seen in the eyepiece under an optical microscope with a 10× lens and a 40× objective lens.

TNF-α, IL-10, and IL-1β in plasma and colon were determined. In the colon homogenate, the data were shown as pg cytokines per mg of total protein content.

Immunohistochemistry Assay

Colon tissue slices were stained with immunohistochemistry in accordance with the technique to look for the expression in the tissues of the colon of the inflammatory pathway proteins TLR4, MyD88, and NF-B p65. After being washed with PBS three times and 5% BSA to stop the overproduction of protein, the paraffin slices were treated with confined solutions for 10 min to stop endogenous peroxidase activity. Primary antibodies were incubated with the sections for two hours. The appropriate secondary antibody was added, the incubation was maintained for 20 minutes, and then three washes with PBS were performed for three minutes each. Following counterstaining with hematoxylin, the slides underwent coloring using a DAB chromogenic reagent. The parts were then examined under a microscope after being sealed with neutral gum.

Western Blotting

Using RIPA lysis buffer with protease to prepare the total protein inhibitor, the homogenates were split on ice for 30 minutes, shaking once every 5 minutes to ensure complete cleavage. The supernatant was collected after two centrifugations at 12,000 rpm for ten minutes at 4 °C. The BCA protein assay kit was used to measure the protein concentrations, which were then diluted to the same level. Then, MUC-2, ZO-1, Occludin, TLR4, MyD88 and NF-κB p65 in colon homogenate were isolated by WB, and their expressions were detected and quantified by the Alpha software processing system.

Gut Microbiota Sequencing

In accordance with the manufacturer's instructions, total genomic DNA was collected from rat faeces samples using the soil/ DNA faeces magnetic kit in guide t96. The highly variable v3-v4 region of the 16S rRNA of the bacterium was amplified using initiators for 806R: 5 "-actcctacggtgcagca-3" and 338F: 5 "-actcctacggtgcagca-3". The PCR products were tested on agarose gel and purified with the Omega DNA purification kit. The purified PCR products were collected and tested on the Illumina Novaseq 6000 platform.

Using USEARCH (version 10.0), qualifying sequences that met the 97% similarity criteria were assigned to a single operational taxonomic unit (OTU). With a confidence level of 70%, taxonomic annotation of OTUs/ASVs was made in QIIME2[17] using the SILVA database[18] (version 138.1) and the Naive Bayes classifier. Using the QIIME2 program, alpha was used to determine the complexity of species diversity in each sample. To assess sample diversity for species complexity, PCoA was used to study estimates of beta diversity. The quantity and diversity of microorganisms were compared using a unidirectional analysis of variance. Differentially abundant taxa were evaluated using linear discriminant analysis (LDA) and effect size (LEfSe). The analysis of the sequencing was done using the web-based tool BMKCloud (www.biocloud.net).

Statistical Analysis

All statistical analyses were performed via SAS 8.2 and data were expressed as mean±SD. ANOVA was used to analyze multiple groups, and variance describes a uniform normal distribution of data. The mean separation was statistically significant using the LSD test, $P<0.05$. Nonparametric test was used when one or more series were not normally distributed. Scoring data were analyzed using a non-parametric test (Kruskal–Wallis H rank sum test), and data were represented by Md (P25, P75).

Results

XLZXT Improves the Clinical Manifestations of DSS-Induced UC

The clinical symptoms of low vitality, diarrhea, body weight loss and hematochezia were substantially more pronounced in the DSS-treated colitis mice than in the control group (P<0.05), as shown in Figure 2A, and these symptoms led to a higher DAI score. These symptoms were alleviated and the DAI scores in the mesalazine and XLZXT-M groups were considerably lower (P<0.05) with the use of mesalazine and XLZXT as treatments (Figure 2B).

A significant predictor of the severity of colitis is colon length.[19] The length of colon in the DSS group was significantly shorter than the control group (P<0.05). Both the mesalazine and XLZXT-M groups significantly differed from the DSS group (P<0.05). (Figure 2C and D)

Hyperplasia of the spleen is also a characteristic symptom in UC mice. The spleen indices were higher in the DSS group compared to the control group, as indicated in Figure 2E (P<0.01). When compared to the DSS group, the spleen indices in mesalazine, XLZXT-L, XLZXT-M and XLZXT-H groups were significantly decreased in comparison with the DSS group (P<0.05).

Histopathology

Compared with the control group, DSS induced colonic mucosal epithelial injury or detachment, lots of inflammatory cells infiltrated into the submucosa, the intestinal glands were significantly enlarged, the number of common crypts was significantly reduced, the intestinal submucosa was edematous and thickened, and the crypts were distorted and atrophied (Figure 2F). Mesalazine or XLZXT was improved after the intervention. Compared with the blank group, the CMDI score of DSS group increased significantly. After drug intervention, compared with the DSS group, the CMDI scores of mesalazine, XLZXT-M and XLZXT-H group were decreased significantly (P<0.01). The CMDI scores of the XLZXT-L dose group also showed a downward trend, but no statistically significant change (P>0.05, Figure 2G).

The colonic mucosal epithelium of the DSS group was incomplete compared to the control group, the goblet cells were arranged irregularly, the number was reduced, destroyed, or even disappeared, the majority of them were vacuolar, and the glycogen mucous substances were severely reduced and released into the intestinal glands (Figure 2H). Mesalazine or XLZXT levels improved following the intervention. The number of goblet cells in the DSS group was much lower than in the control group, and the difference was statistically significant (P<0.01). Compared to the DSS group, the number of goblet cells in the mesalazine, XLZXT-M, and XLZXT-H groups rose considerably (P<0.01); the number of goblet cells in the XLZXT-L group tended to rise (P>0.05, Figure 2I).

XLZXT Alleviated DSS-Induced Inflammatory Response

TNF-α, IL-1β and IL-6 levels in plasma and colons were considerably elevated, as shown in Figure 3, whereas in comparison to the control group, the DSS group had decreased levels of the anti-inflammatory cytokine IL-10 expression (P<0.01). Mesalazine and XLZXT, on the other hand, significantly controlled the heightened levels of pro-inflammatory cytokines and reduced expressions of anti-inflammatory cytokines. All the findings demonstrated that XLZXT had a notable anti-inflammatory impact in the mice model of colitis brought on by DSS (Figure 3).

XLZXT Improved Intestinal Barrier Function

The expression levels of the proteins MUC-2, ZO-1, and Occludin in the model group were considerably lower than those in the blank group, according to Western blotting analysis (P<0.05). Following XLZXT treatment, MUC-2 protein

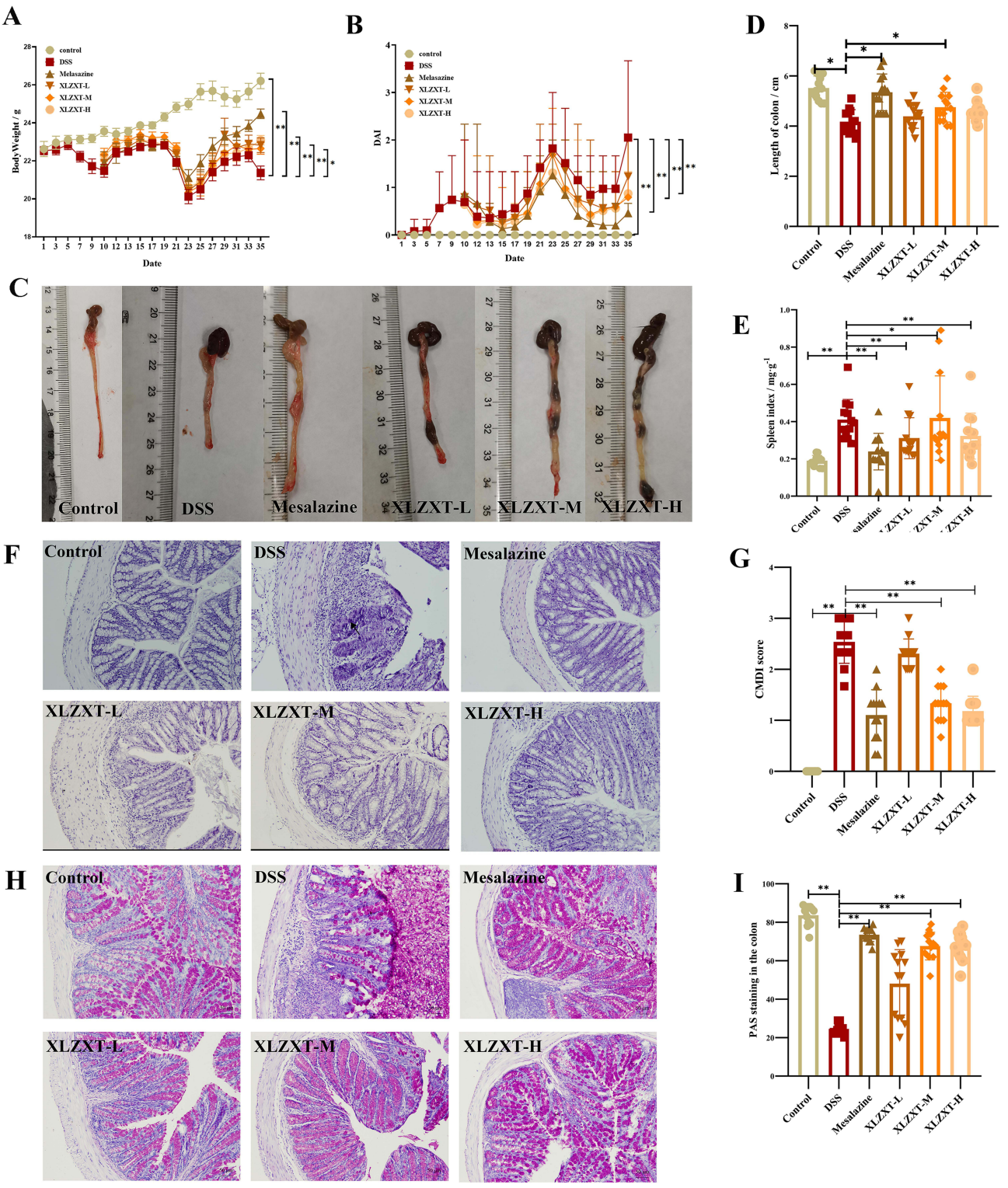

Figure 2 XLZXT improves the symptoms of DSS-induced UC. (**A**) Colon images of different groups. (**B**) Histogram statistical of colon length. (**C**) Curve chart of mice body weight across time. (**D**) Curve chart of DAI scores of mice. (**E**) Histogram statistical of spleen index. (**F**) Representative of H&E staining of colonic sections, ×200. The black arrow means the site of neutrophil immersion. (**G**) Histogram statistical of CMDI scores. (**H**) Representative of PAS staining of colonic sections, ×200. (**I**) Histogram statistical of PAS staining in the colon. Data are expressed as mean ±SD (n=12 in control group, n=13 in other groups). *P<0.05, **P<0.01.

expression was considerably elevated in the XLZXT-M and XLZXT-H groups (P<0.05); ZO-1 and Occludin protein expression was considerably elevated in the XLZXT-L group and XLZXT-M group in comparison to the DSS group (P<0.05) (Figure 4A–D).

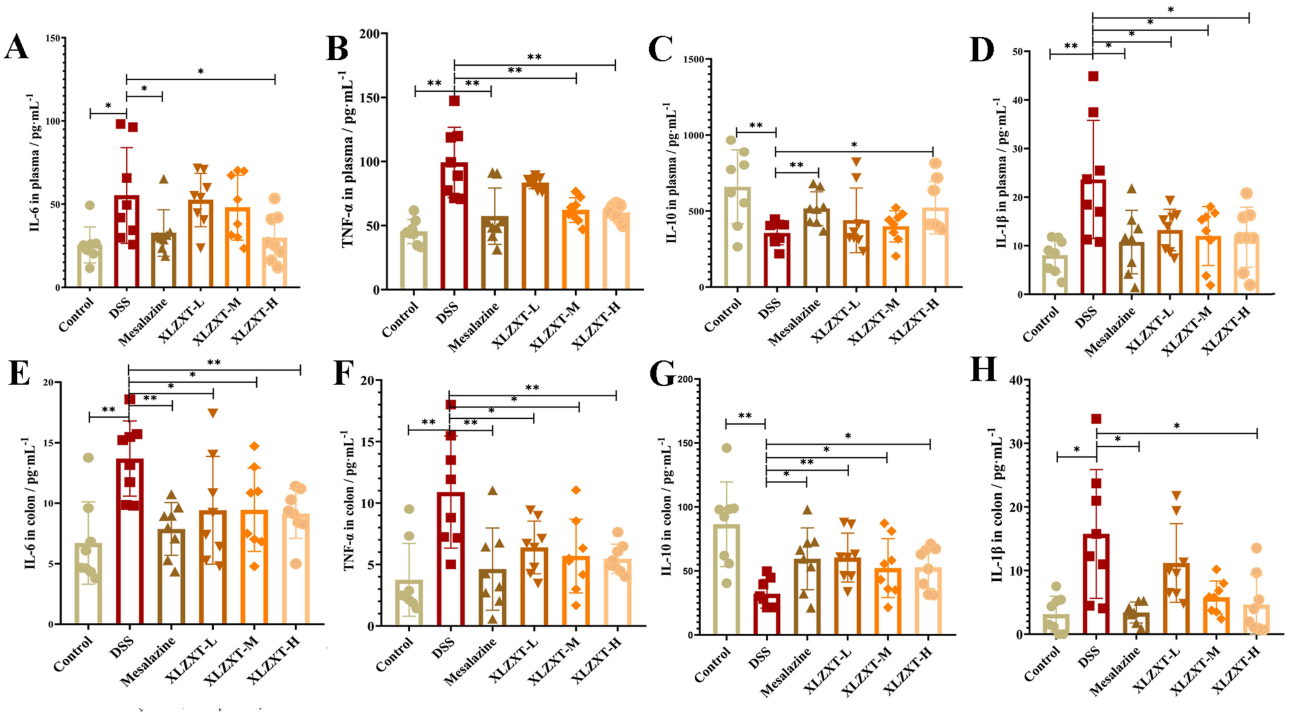

Figure 3 Concentrations of cytokines in plasma and colon. (**A**) Histogram statistical of IL-6 in plasma. (**B**) Histogram statistical of TNF-α in plasma. (**C**) Histogram statistical of IL-10 in plasma. (**D**) Histogram statistical of IL-1β in plasma. (**E**) Histogram statistical of IL-6 in colon. (**F**) Histogram statistical of TNF-α in colon. (**G**) Histogram statistical of IL-10 in colon. (**H**) Histogram statistical of IL-1β in colon. Data are expressed as mean±SD (n=8). *P<0.05, **P<0.01.

The Effects of XLZXT on TLR4-MyD88-NF-κB Signaling Pathway

According to IHC results, TLR4 was mainly distributed in the cell membrane and cytoplasm, MyD88 was mainly distributed in the surface of the colon mucosa, the cytoplasm of cells in the submucosa and lamina propria, and NF-κB p65 was mainly distributed in the nucleus and cytoplasm of the colon (Figure 4E). Compared with the control group, the relative expression level of TLR4, MyD88 and NF-κB p65 in the DSS group was significantly increased (P<0.05, P<0.01, P<0.01). Both the mesalazine and the XLZXT-H significantly reduced the relative expression level of MyD88 in colon tissue when compared to the DSS group, the relative expression level of TLR4 was considerably reduced in mesalazine, XLZXT-M and the XLZXT-H groups when compared to the DSS group (P<0.05, Figure 4F–H).

The colon of DSS group had substantially higher levels of TLR4 protein expression compared to the control group (P<0.01). The expression of TLR4 in colon tissue was considerably reduced by mesalazine, XLZXT-L, and XLZXT-M when compared to the DSS group (P<0.01). TLR4 expression in XLZXT-L group showed a tendency to decline (P>0.05). The DSS group's colon tissue had much higher expression of MyD88 than the control group did, and this difference was statistically significant (P<0.05). Both the mesalazine and the XLZXT-H significantly reduced the expression level of MyD88 in colon tissue when compared to the DSS group (P<0.05). Both XLZXT-L and XLZXT-M groups tended to lower (P>0.05) the amount of MyD88 expression. The DSS group's colon tissue had significantly higher levels expression of NF-κB p65 than control group, and the difference was statistically significant (P<0.01). Mesalazine and the XLZXT-H group were able to considerably lower the expression of the NF-κB p65 protein when compared with the DSS group, and this difference was statistically significant (P<0.01, or P<0.05); the XLZXT-L and XLZXT-M group tended to do so (P>0.05) (Figure 4I–L).

Diversity Analysis of Gut Microbiota Sequencing Data

Alpha diversity reflects the species richness and species diversity of a single sample (Figure 5A–D). The Simpson index of DSS group was significantly increased (P<0.05), the Shannon index showed an increasing trend (P>0.05), while the ACE index and Chao1 index showed a decreasing trend (P>0.05) compared with the control group. The Shannon index and Simpson index in the mesalazine group, XLZXT-M group and XLZXT-H group were significantly decreased

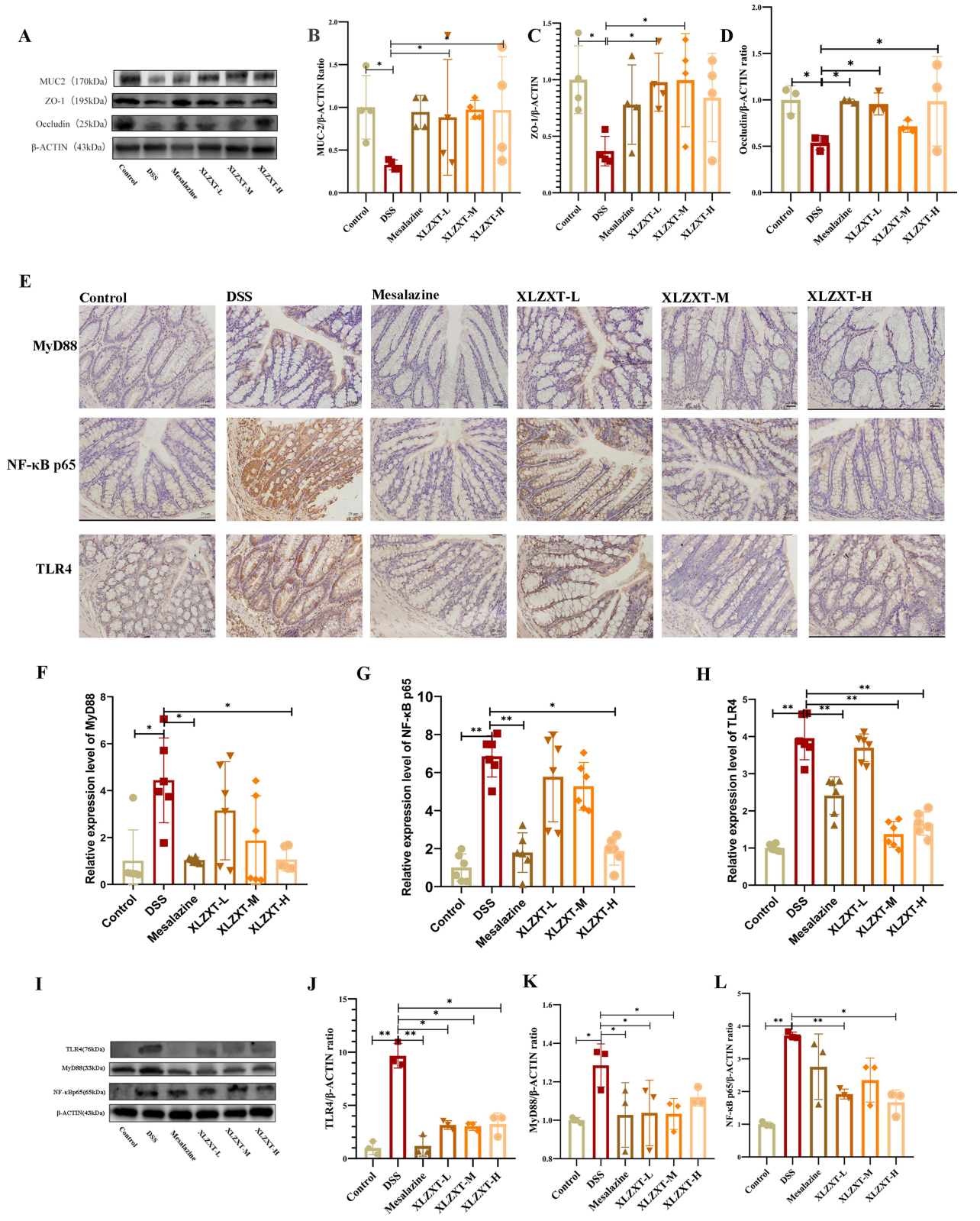

Figure 4 The effects of XLZXT on the TLR4-MyD88-NF-B signaling pathway and repairing the intestinal mucosa barrier. (**A**) The expression of MUC2, ZO-1 and Occludin in the colon by the WB. (**B**–**D**) Histogram statistical of the expression of MUC2, ZO-1 and Occludin in the colon by the WB. Data are expressed as mean ±SD (n=4 in each group). *P<0.05, **P<0.01. (**E**) The expression of -MyD88, NF-κB and TLR4 in the colon by the IHC, ×400. (**F**–**H**) The relative expression level of -MyD88, NF-κB and TLR4 in the colon by the IHC. Data are expressed as mean ±SD (n=6 in each group). *P<0.05, **P<0.01. (**I**) The expression of MyD88, NF-κB and TLR4 in the colon by the WB. (**J**–**L**) Histogram statistical of the expression of MyD88, NF-κB and TLR4 in the colon by the WB. Data are expressed as mean ±SD (n=3 in each group). *P<0.05, **P<0.01.

compared with the DSS group (P<0.05). The Shannon index and Simpson index of the XLZXT-L group showed a decreasing trend compared with the model group (P>0.05). And the ACE index and Chao1 index of mice in the XLZXT-L group and XLZXT-M group were significantly increased compared with the DSS group (P<0.05). And the mesalazine group and the XLZXT-H group showed a trend of increasing ACE index and Chao1 index compared with DSS group (P>0.05). The results of dilution curve and aroma concentration curve showed that the index was accurate and the data sequencing was sufficient to extract most microbial data from the sample (Figure 5E and F).

Venn diagram was used to show the number of common and unique features between samples. There were 356 OTU units in the blank group and the model group, 2 OTUs were unique to the blank group, and 10 OTUs were unique to the model group. There were 364 OTU units in the mesalazine group and the model group, one OTU unit was unique to the mesalazine group, and two OTU units were unique to the model group. There were 363 OTU units in the XLZXT-L group and the model group, 2 OTU units were unique to the XLZXT-L group, and 3 OTU units were unique to the model group. There were 363 OTU units in the XLZXT-M group and the model group, 3 OTU units were unique to the XLZXT-M group, and 3 OTU units were unique to the model group. There were 360 OTU units in the XLZXT-H group and the model group, one OTU unit was unique to the XLZXT-H group, and six OTU units were unique to the model group (Figure 5G).

Based on PLS-DA method, the structure of intestinal flora in each group was analyzed by Beta method. As shown in Figure 5H, the distance between sample points was negatively correlated with the similarity of intestinal flora structure. The distance between samples in each group was small, and the similarity within the group was large, indicating that the difference within the group was small. The distance between the blank group and the model group was large, and the similarity between the groups was small, indicating that the intestinal flora structure of the two groups of mice was very different. Compared with the distance between the model group and the mesalazine group and the XLZXT group, the distance between the model group and the high dose group of XLZXT was the farthest, followed by the middle dose group of XLZXT, and finally the low dose

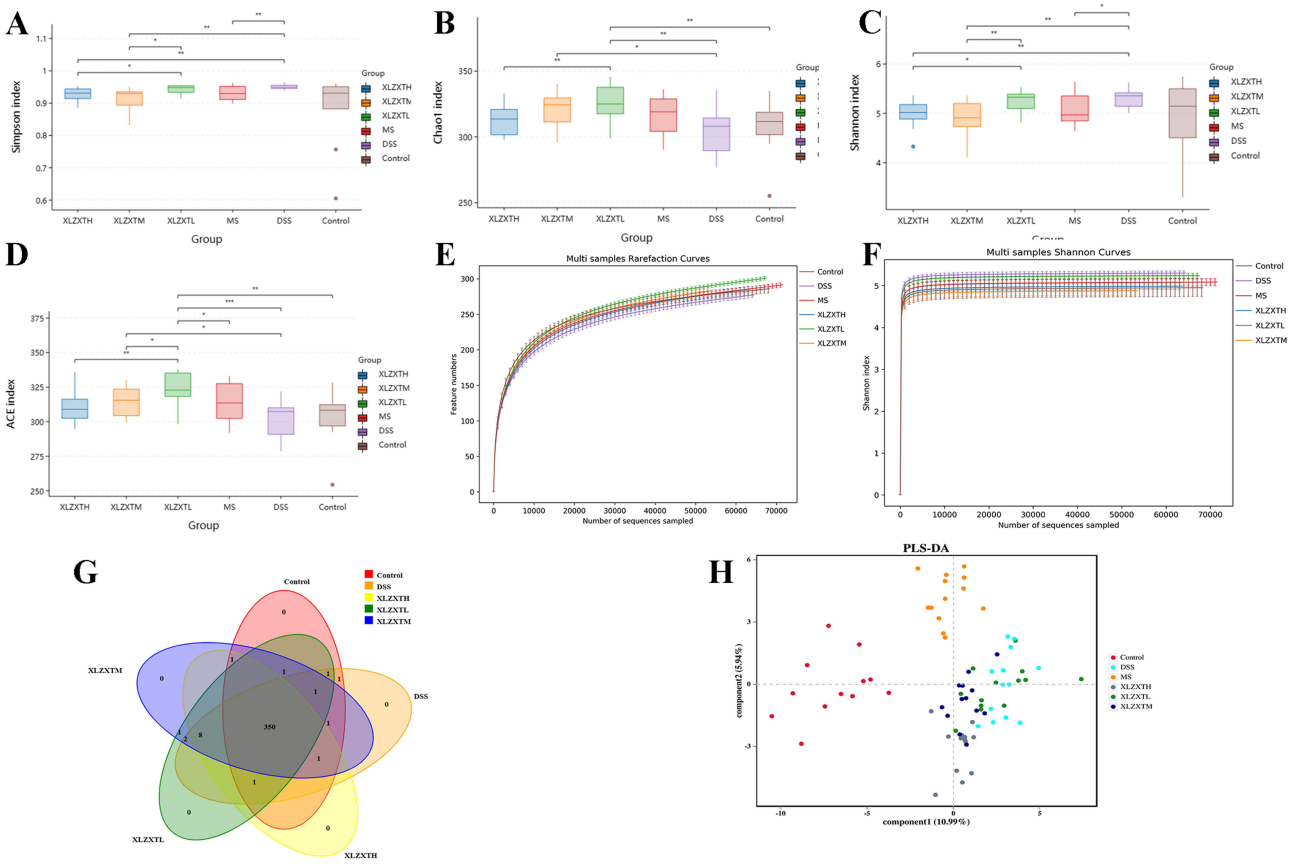

Figure 5 Effect of XLZXT on gut microbiota diversity. (**A**–**F**) Alpha diversity index of observed species, Simpson, Chao 1, Shannon, ACE, Rarefaction Curve, Shannon Curve. (**G**) Venn diagram of OUTS in different groups. (**H**) PLS-DA analysis of species in different groups.*P<0.05, **P<0.01, ***P<0.001.

group of XLZXT and the mesalazine group. The farther the distance between the model group and each group, the smaller the similarity between the groups, and the more obvious the difference in the intestinal flora structure of the mice between the groups. XLZXT alleviated the symptoms of UC mice might be related to the intestinal flora structure of UC mice. The changes in the flora structure of the XLZXT group and the mesalazine group may be different.

Analysis of Intergroup Differences in Gut Microbiota

The abundances of Bacteroidaceae, Clostridium, Erysipelotrichaceae, Marinilabiliaceae, PeptoStreptococcaceae, Rikenellaceae, Burkholderiaceae, Fusobacteriaceae, Enterobacteriaceae and Marinifilaceae in the DSS group were increased significantly ($P<0.05$), and the abundances of Lactobacillaceae and Muribaculaceae were decreased significantly compared with the control group ($P<0.05$). The abundances of Christensenellaceae and Marinilabiliaceae were increased significantly in the XLZXT-L group ($P<0.05$) compared with the DSS group. And the abundances of Rikenellaceae and Deferribacteraceae decreased significantly compared with the model group ($P<0.05$). The abundances of Christensenellaceae and Ruminococcaceae in the XLZXT-M group were increased significantly compared with the DSS group ($P<0.05$). And the abundances of Desulfovibrionaceae, Erysipelotrichaceae, Bacteroidaceae and Marinilabiliaceae were decreased significantly compared with the DSS group ($P<0.05$). The abundances of Marinilabiliaceae, Erysipelotrichaceae, Clostridiaceae, PeptoStreptococcaceae, Enterococcaceae, Enterobacteriaceae and Bacteroidaceae in the XLZXT-H were decreased significantly compared with the model group ($P<0.05$). The main differences of gut microbiota in each group in terms of family and species are shown in Figure 6A–D. LEfSe can realize the comparison between two or more groups, as well as the comparison between subgroups within groups, so as to find biomarker with statistical difference between different groups (Figure 6E).

Correlation Analysis of Gut Microbiota with Inflammatory Factors and Intestinal Mucosal Proteins

The relative abundance of Lactobacillaceae was positively correlated with the expression of intestinal mucosal proteins MUC-2 and Occludin ($P<0.05$; Figure 6F). The relative abundance of Desulfovibrionaceae was negatively correlated with the expression level of ZO-1 protein ($P<0.05$). The relative abundance of Deferribacteraceae was negatively correlated with the protein expression of ZO-1 and Occludin ($P<0.05$; Figure 6F). The relative abundance of Erysipelotrichaceae, Clostridium_sp._K4410. MGS-306, PeptoStreptococcaceae, Rikenellaceae and Bacteroidaceae were negatively correlated with the protein expression levels of MUC-2, ZO-1 and Occludin ($P<0.05$; Figure 6F). The relative abundances of Erysipelotrichaceae, Clostridium_sp._K4410. MGS-306, PeptoStreptococcaceae, Rikenellaceae, Burkholderiaceae, Bacteroidaceae and Deferribacteraceae were positively correlated with the expression levels of pro-inflammatory cytokines IL-6, TNF-α and IL-1β ($P<0.05$), and negatively correlated with the expression level of IL-10 ($P<0.05$; Figure 6G). The relative abundance of Lactobacillaceae was negatively correlated with the expression levels of IL-6, TNF-α and IL-1β ($P<0.05$), and positively correlated with the expression level of IL-10 ($P<0.05$; Figure 6G).

Discussion

In clinics, XLZXT is mostly used to treat conditions of the digestive tract. Some clinical study has shown that XLZXT is used alone or in combination for the treatment of ulcerative colitis, and it has played a significant effect. In this study, it was found that it has a good therapeutic effect on DSS-induced UC mice. XLZXT Tablet can alleviate the symptoms of weight loss, loose stools, bloody stools and shortened colon length in UC mice, and has a certain anesis and repair effect on colon histopathological damage in UC mice; it can down-regulate pro-inflammatory cytokines. The expression levels of IL-6, IL-1β and TNF-α were down-regulated, while the expression of the anti-inflammatory cytokine IL-10 was up-regulated. Together, these results reveal that XLZXT is effective for DSS-induced colitis. Notably, XLZXT-H (2716.2 mg/kg) was found to exert similar effect to mesalazine (310.0 mg/kg).

Colonic mucus is mainly composed of MUC-2, which is distributed throughout the normal human digestive tract and is most expressed in the colon of healthy humans. MUC-2 protein showed a low expression state. Occludin protein is an important transmembrane protein that constitutes TJ protein and is responsible for regulating the stability and permeability of tight junctions.[20] ZO-1 protein forms a stable linking complex between Occludin protein and actin protein,

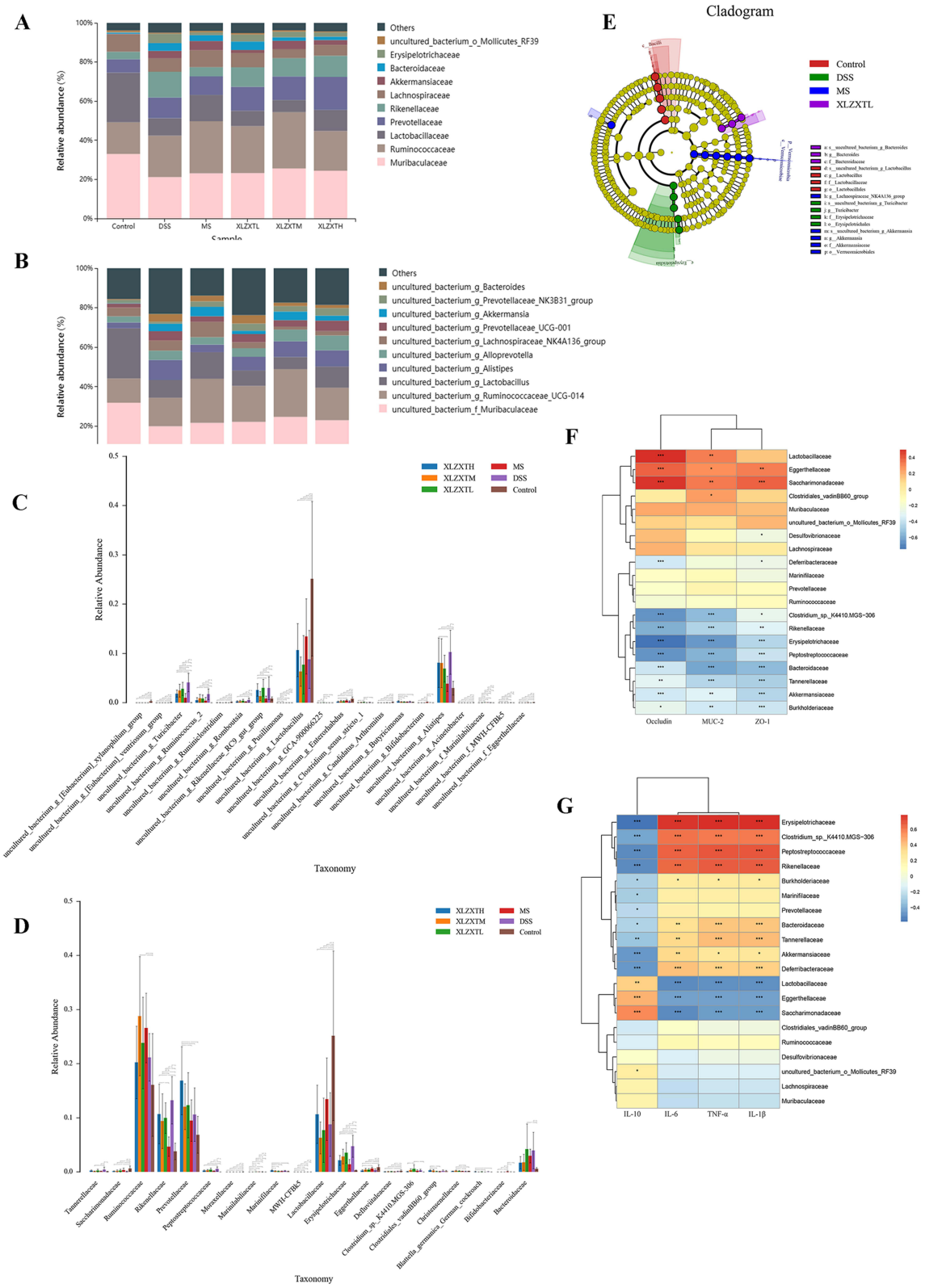

Figure 6 The effects of XLZXT on regulating the gut microbiota. (**A** and **B**) Bar chart of the relative abundance of the bacterial flora in species and family. (**C** and **D**) Histogram statistical of species and families in different groups. (**E**) Evolutionary branch map of LEfSe analysis. (**F** and **G**) Heatmap for correlation analysis between gut microbiota and the expression of MUC2, ZO-1, Occludin, IL-10, IL-6, TNF-α and IL-1β. Data are expressed as mean±SD (n=4 in each group). *P<0.05, **P<0.01, ***P<0.001.

which has the effect of preventing the entry of harmful substances and pathogens.[21] The research results show that XLZXT can increase the expression levels of intestinal mucosal proteins MUC-2, Occludin and ZO-1, indicating that it can relieve the symptoms of UC by repairing the colonic mucosal barrier and play a therapeutic effect.

More and more evidences have shown that the inflammatory response is mainly regulated by the TLR4-MyD88-NF-κB pathway. Toll-like receptors (TLRs) are transmembrane proteins that share an outer membrane domain rich in leucine repeats and play a central role in identifying and responding to microbial pathogens and maintaining the integrity of the intestinal epithelial barrier. Toll-like receptor 4 (TLR4) is an important member of the toll-like receptor family, mainly expressed in the distal colon.[22] As a key upstream factor of MyD88/NF-κB signaling pathway, intestinal innate immune response induced by external stimulation can up-regulate TLR4 expression through MyD88-dependent signaling pathway, thereby activating NF-κB and leading to inflammatory response.[23] The ubiquitination and degradation of TLR4 were elicited to relieve inflammatory disorders.[24] Studies have shown that when pathogenic microorganisms, bacteria and antigens activate TLR4, the TLR4 domain binds to the carboxy terminus of MyD88 and activates downstream signaling molecules MyD88 and TRAF-6 by recognizing pathogen-related molecular patterns. The serine-threonine protein kinase IRAK downstream of MyD88 is phosphorylated, and the phosphorylated IRAK binds to TRAF6 and further activates NF-κB.[24–27] NF-κB is a crucial nuclear transcription factor that controls immunological and inflammatory responses as well as many cellular reactions in the body. After NF-κB is activated, immune cells such as dendritic cells and monocytes mediate the inflammation and immune response of the intestinal mucosa, and at the same time secrete pro-inflammatory factors, mucosal damage.[28,29] The experimental results show that XLZXT can significantly inhibit the overexpression of NF-κB p65, MyD88 and TLR4 in DSS-induced UC mice ($P<0.05$). This suggested that the response might inhibit inflammation by regulating TLR4-MyD88-NF-κB signaling pathway, thereby alleviating the inflammatory symptoms of UC and exerting a therapeutic effect.

There are a large number of microorganisms in the gut, with a wide variety and a large number, most of which are anaerobic bacteria. At the phylum level, it can be divided into four categories: Bacteroidetes, Firmicutes, Actinobacteria and Proteobacteria. In terms of function, it can be divided into three categories: beneficial bacteria, symbiotic bacteria and harmful bacteria.[30] In the normal body, gut microbiota is in homeostasis. However, in UC patients, the intestinal mucosal barrier function is damaged, the balance between gut microbiota is broken, and the flora stimulates intestinal epithelial cells and induces intestinal inflammation.

Studies have shown that after patients are infected with Clostridiaceae, IL-21 and IFN-γ in vivo jointly stimulate T cells, induce inflammatory signal transduction, activate transcription factors, and then induce interferon gene expression.[31] Erysipelotrichaceae has to be found can affect the expression level of inflammatory cytokine TNF-α, induce the activation of NF-κB and STAT3 signaling pathways, and lead to colon inflammation by increasing the expression level of TNF-α. Peptostreptococcaceae can affect intestinal barrier function.[32] Rikenellaceae is closely related to colorectal cancer.[33] In the investigation, the abundance of Rikenellaceae in patients with pathological incomplete response was significantly higher than that in patients with pathological complete response.[34] Studies have shown that the increase of Deferribacteraceae in the intestine can lead to the imbalance of intestinal mucin and intestinal inflammation, and even induce the formation of tumors.[35] In this study, correlation analysis showed that the relative abundance of these bacteria was positively correlated with the expression levels of pro-inflammatory cytokines IL-6, TNF-α and IL-1β ($P<0.05$). It was negatively correlated with the expression of anti-inflammatory cytokine IL-10, intestinal mucosal proteins MUC-2, ZO-1 and Occludin ($P<0.05$). It was found that the relative abundance of these florae in DSS group was significantly increased ($P<0.05$) and the relative abundance of these florae was significantly decreased under the intervention of different doses of XLZXT ($P<0.05$). Therefore, the therapeutic effect of XLZXT on DSS-induced UC mice may be related to the effects of Bacteroidaceae, Clostridiaceae, Erysipelotrichaceae, PeptoStreptococcaceae, Rikenellaceae, Bacteroidaceae, Clostridiaceae, Erysipelotrichaceae, Peptostreptococcaceae, and Rikenellaceae. The relative abundance of Rikenellaceae and Deferribacteraceae further affects intestinal inflammatory factors, intestinal mucosal proteins and intestinal barrier function.

Bacteroidaceae in Bacteroidetes can produce sphingolipids. In normal organisms, bacterial sphingolipid is conducive to intestinal health and maintains intestinal dynamic balance.[36,37] Some pathogenic bacteria from Bacteroidaceae can have adverse effects on the body. For example, Bacteroides fragilis has the properties of inducing colon abscesses. Excessive secretion of Bacteroides Fragilis in the colon can easily cause crypt abscesses and promote the further expansion of colon inflammation. Bacteroides thetaiotaomicron can promote the growth of pathogenic bacteria. In the process of colon inflammation and ulcer development, intestinal mucosal permeability will increase and pathogenic bacteria will invade intestinal epithelial cells and cause increased inflammation. Bacteroides fragilis producing enterotoxin has the effect of inducing human diseases, secreting

enterotoxin, stimulating intestinal mucosa and triggering UC[38] In addition, Proteobacteria, Marinilabiliaceae.[39] Enterobacteriaceae,[40] Desulfovibrionaceae,[41] Enterococcaceae and other harmful bacteria can destroy the intestinal mucosal barrier by secreting endotoxins or causing gut microbiota disorder, affecting intestinal mucosal permeability and thus causing colon inflammation. Firmicutes,[42] Actinobacteria, Ruminococcaceae,[43] Christensensllaceae[44] and other probiotics can reduce the adhesion of harmful bacteria on colon mucosa, inhibit the growth and reproduction of pathogenic microorganisms in the intestine and stimulate the production of immunoglobulin can reduce intestinal permeability, protect the integrity of intestinal barrier and relieve UC symptoms. As the result show, Shannon index and Simpson index of the DSS group have increased compared with the control group. The Shannon index and Simpson index of the XLZXT-M group and XLZXT-H group showed a significant decrease compared with the model group ($P<0.05$). Compared with the control group, the ACE index and Chao1 index of the model group were decreased, while compared with the DSS group, the ACE index and Chao1 index of the XLZXT-L and XLZXT-M groups were significantly increased ($P<0.05$). In addition, under XLZXT treatment, the relative abundance of the above harmful bacteria was significantly decreased ($P<0.05$), while the relative abundance of probiotics was significantly increased ($P<0.05$). The results indicated that the therapeutic effect of XLZXT on UC mice may reduce the adhesion of intestinal harmful bacteria, increase the abundance of beneficial bacteria, relieve gut microbiota disorder and promote the restoration of intestinal microecological balance, so as to further play a therapeutic role.

Conclusion

In this study, we investigated the efficacy and mechanisms of XLZXT in treating UC through the DSS-induced chronic UC model mice. To the best of our knowledge, this is the first study to probe the therapeutic potential of XLZXT for UC. Our findings indicated that XLZXT could effectively alleviate the clinical symptoms of UC and in-depth apparently modify the the levels of relevant cytokines in the organism to maintain the system homeostasis. Specifically, our results suggested that XLZXT might treat DSS-induced UC by repairing the intestinal mucosa barrier, regulating the TLR4/MyD88/NF-κB p65 signaling pathway, and restoring gut microbiota balance.

Abbreviations

Akt, Protein kinase B; MUC-2, Mucoprotein-2; BSA, Bovine serum albumin; MyD88, Myeloiddifferentiationfactor88; CD, Crohn's disease; IL-10, Interleukin-10; CD-14, Endotoxin receptors on Kupffer cell membrane-14; IL-12, Interleukin-12; CMDI, Colon mucosa damage index; JAK2, Janus kinase 2; CRP, C-reactive protein; LPS, Lipopolysaccharide; DAI, Disease activity index; IP-10, Interferon-inducible protein-10; DSS, Dextran sulfate sodium; NC, Nitrocellulose filter membrane; ECL, Enhanced chemiluminescence; NLRP3, Nucleotide-binding oligomerization domain-like receptor protein 3; Elisa, Enzyme-linked immunosorbent assay; NF-κB, Nuclear factor-kappa B; HE, Hematoxylin-eosin; OD, Optical density; HRP, Horseradish peroxidase; OUT, Operational taxonomic units; IBD, Inflammatory bowel disease; PAS, Periodic acid-schiff; IFN-γ, Interferon gamma; PBS, Phosphate buffered saline; IHC, Immunohistochemistry; PCoA, Principal co-ordinates analysis; IL-1β, Interleukin-1β; PCR, Polymerase chain reaction; IL-6, Interleukin-6; PMSF, Pheny methane sulfonyl fluoride; MD-2, Myeloid differentiation protein-2; PRRs, Pathogen-associated molecular pattern; MPO, Myeloperoxidase.Abbreviations: Akt, Protein kinase B; MUC-2, Mucoprotein-2; BSA, Bovine serum albumin; MyD88, Myeloiddifferentiationfactor88; CD, Crohn's disease; IL-10, Interleukin-10; CD-14, Endotoxin receptors on Kupffer cell membrane-14; IL-12, Interleukin-12; CMDI, Colon mucosa damage index; JAK2, Janus kinase 2; CRP, C-reactive protein; LPS, Lipopolysaccharide; DAI, Disease activity index; IP-10, Interferon-inducible protein-10; DSS, Dextran sulfate sodium; NC, Nitrocellulose filter membrane; ECL, Enhanced chemiluminescence; NLRP3, Nucleotide-binding oligomerization domain-like receptor protein 3; Elisa, Enzyme-linked immunosorbent assay; NF-κB, Nuclear factor-kappa B; HE, Hematoxylin-eosin; OD, Optical density; HRP, Horseradish peroxidase; OUT, Operational taxonomic units; IBD, Inflammatory bowel disease; PAS, Periodic acid-schiff; IFN-γ, Interferon gamma; PBS, Phosphate buffered saline; IHC, Immunohistochemistry; PCoA, Principal co-ordinates analysis; IL-1β, Interleukin-1β; PCR, Polymerase chain reaction; IL-6, Interleukin-6; PMSF, Pheny methane sulfonyl fluoride; MD-2, Myeloid differentiation protein-2; PRRs, Pathogen-associated molecular pattern; MPO, Myeloperoxidase.

Ethics Statement

All experimental procedures were conducted in accordance with "Guidelines for the Management and Use of Laboratory Animals" (Ministry of Science and Technology, China, 2006), and the study was approved by Experimental Animal Ethics Committee of the Research Institute of Beijing Tongrentang Co. LTD with the ethical approval number YJY-2021-030904.

Acknowledgments

This work is supported by the National Key R&D Program of China. We deeply appreciate all the members of our team.

Author Contributions

All authors contributed to data analysis, drafting or revising the article, have agreed on the journal to which the article will be submitted, gave final approval of the version to be published, and agree to be accountable for all aspects of the work.

Funding

This work was supported by National key research and development program (2019YFC1711400).

Disclosure

The authors report no conflicts of interest in this work.

References

1. Kobayashi T, Siegmund B, Le Berre C, et al. Ulcerative colitis. *Nat Rev Dis Primers*. 2020;6(1):74. doi:10.1038/s41572-020-0205-x
2. Du L, Ha C. Epidemiology and pathogenesis of ulcerative colitis. *Gastroenterol Clin North Am*. 2020;49(4):643–654. doi:10.1016/j.gtc.2020.07.005
3. Rogler G. Chronic ulcerative colitis and colorectal cancer. *Cancer Lett*. 2014;345(2):235–241. doi:10.1016/j.canlet.2013.07.032
4. Flynn S, Eisenstein S. Inflammatory bowel disease presentation and diagnosis. *Surg Clin North Am*. 2019;99(6):1051–1062. doi:10.1016/j.suc.2019.08.001
5. Brown K, DeCoffe D, Molcan E, Gibson DL. Diet-induced dysbiosis of the intestinal microbiota and the effects on immunity and disease. *Nutrients*. 2012;4(8):1095–1119. doi:10.3390/nu4081095
6. Ungaro R, Mehandru S, Allen PB, Peyrin-Biroulet L, Colombel J-F. Ulcerative colitis. *Lancet*. 2017;389(10080):1756–1770. doi:10.1016/S0140-6736(16)32126-2
7. Raine T, Bonovas S, Burisch J, et al. ECCO guidelines on therapeutics in ulcerative colitis: medical treatment. *J Crohns Colitis*. 2022;16(1):2–17. doi:10.1093/ecco-jcc/jjab178
8. Spinelli A, Bonovas S, Burisch J, et al. ECCO guidelines on therapeutics in ulcerative colitis: surgical treatment. *J Crohns Colitis*. 2022;16(2):179–189. doi:10.1093/ecco-jcc/jjab177
9. Paridaens K, Fullarton JR, Travis SPL. Efficacy and safety of oral Pentasa (prolonged-release mesalazine) in mild-to-moderate ulcerative colitis: a systematic review and meta-analysis. *Curr Med Res Opin*. 2021;37(11):1891–1900. doi:10.1080/03007995.2021.1968813
10. Salice M, Rizzello F, Calabrese C, Calandrini L, Gionchetti P. A current overview of corticosteroid use in active ulcerative colitis. *Expert Rev Gastroent*. 2019;13(6):557–561. doi:10.1080/17474124.2019.1604219
11. Roggenbrod S, Schuler C, Haller B, et al. Patient perception and approval of fecal microbiota transplantation (FMT) as an alternative treatment option for ulcerative colitis. *Z Gastroenterol*. 2019;57(3):296–303. doi:10.1055/a-0821-7166
12. Yan S, Zhang LL. Diagnosis and treatment of ulcerative colitis based on "body-disease-syndrome differentiation". *Tianjin Tradit Chin Med*. 2020;10(37):4.
13. Wang B, Cui S, Wang H. Professor Chen Zhishui's clinical experience in the treatment of ulcerative colitis. *Chin J Integr Traditional West Med Diges*. 2008;2008(02):112–114.
14. Wang Beichen CS, Wang H. Forty-four cases with ulcerative colitis of large intestinal damp-heat syndrome treated with xianglian zhixie tablets. *Henan Tradit Chin Med*. 2015;35(09):2179–2181.
15. Xi W, Jun Y, Ying L, Qiang Z. Sweet even antidiarrheal piece of internal and joint colon ning 43 cases of clinical observation enema treatment of ulcerative colitis. *New Chin Med*. 2015;47(08):64–65.
16. Wirtz S, Popp V, Kindermann M, et al. Chemically induced mouse models of acute and chronic intestinal inflammation. *Nat Protoc*. 2017;12(7):1295–1309. doi:10.1038/nprot.2017.044
17. Bolyen E, Rideout JR, Dillon MR, et al. Reproducible, interactive, scalable and extensible microbiome data science using QIIME 2. *Nat Biotechnol*. 2019;37(8):852–857. doi:10.1038/s41587-019-0209-9
18. Quast C, Pruesse E, Yilmaz P, et al. The SILVA ribosomal RNA gene database project: improved data processing and web-based tools. *Nucleic Acids Res*. 2013;41(Database issue):D590–6. doi:10.1093/nar/gks1219
19. Wang YF, Liu JJ, Huang ZW, et al. Coptisine ameliorates DSS-induced ulcerative colitis via improving intestinal barrier dysfunction and suppressing inflammatory response. *Eur J Pharmacol*. 2021;896:173912. doi:10.1016/j.ejphar.2021.173912
20. Yao DB, Dai WL, Dong M, Dai CL, Wu SD. MUC2 and related bacterial factors: therapeutic targets for ulcerative colitis. *Ebiomedicine*. 2021;74:103751. doi:10.1016/j.ebiom.2021.103751

21. Xiong CL, Chen X, Zhang PX, Zhong C, Liu XL, Jia B. Based on "reverse flow carrying boat" approach to explore the intervention effect of renshen baidu powder on intestinal mucosal barrier ulcerative colitis in rats. *Modernization Traditional Chin Med Materia Medica World Sci Tech*. 2021;23(7):2285–2293.
22. Yao D, Dong M, Dai C, Wu S. Inflammation and inflammatory cytokine contribute to the initiation and development of ulcerative colitis and its associated cancer. *Inflamm Bowel Dis*. 2019;25(10):1595–1602. doi:10.1093/ibd/izz149
23. Cheng X, Yang YL, Yang H, Wang YH, Du GH. Kaempferol alleviates LPS-induced neuroinflammation and BBB dysfunction in mice via inhibiting HMGB1 release and down-regulating TLR4/MyD88 pathway. *Int Immunopharmacol*. 2018;56:29–35. doi:10.1016/j.intimp.2018.01.002
24. Zhang H, He F, Zhou L, Shi M, Li F, Jia H. Activation of TLR4 induces inflammatory muscle injury via mTOR and NF-kappaB pathways in experimental autoimmune myositis mice. *Biochem Biophys Res Commun*. 2022;603:29–34. doi:10.1016/j.bbrc.2022.03.004
25. Yu H, Huh JW, Bai F, Ha UH. DnaJ-induced TLR7 mediates an increase in interferons through the TLR4-engaged AKT/NF-kappa B and JNK signaling pathways in macrophages. *Microb Pathogenesis*. 2022;165:105465. doi:10.1016/j.micpath.2022.105465
26. Momtaz S, Navabakhsh M, Bakouee N, et al. Cinnamaldehyde targets TLR-4 and inflammatory mediators in acetic-acid induced ulcerative colitis model. *Biologia*. 2021;76(6):1817–1827. doi:10.1007/s11756-021-00725-w
27. Bellver DA, Gil-Benso R, Martinez A, et al. Study of the activation of TLR receptors in neurospheres from glioblastoma cells in vitro. *Ann Oncol*. 2018;29:1.
28. Saber S, Youssef ME, Sharaf H, et al. BBG enhances OLT1177-induced NLRP3 inflammasome inactivation by targeting P2X7R/NLRP3 and MyD88/NF-κB signaling in DSS-induced colitis in rats. *Life Sci*. 2021;270:119123. doi:10.1016/j.lfs.2021.119123
29. Zhang CF, Liu B, Ge YZ, Ma KL, Wang CZ, Yan GM. Therapeutic effect of Dahuang Mudan Decoction on inflammation-related colorectal cancer and its influence on TLR4/MyD88/NF-κB-p65 signaling pathway. *Chin J Immunol*. 2021;37(12):1443–1448.
30. Guo S, Geng W, Chen S, et al. Ginger Alleviates DSS-Induced ulcerative colitis severity by improving the diversity and function of gut microbiota. *Front Pharmacol*. 2021;12:632569. doi:10.3389/fphar.2021.632569
31. Mullineaux-Sanders C, Sanchez-Garrido J, Hopkins EGD, Shenoy AR, Barry R, Frankel G. Citrobacter rodentium-host-microbiota interactions: immunity, bioenergetics and metabolism. *Nat Rev Microbiol*. 2019;17(11):701–715. doi:10.1038/s41579-019-0252-z
32. Chen L, Wilson JE, Koenigsknecht MJ, et al. NLRP12 attenuates colon inflammation by maintaining colonic microbial diversity and promoting protective commensal bacterial growth. *Nat Immunol*. 2017;18(5):541–551. doi:10.1038/ni.3690
33. Wang YN, Meng XC, Dong YF, et al. Effects of probiotics and prebiotics on intestinal microbiota in mice with acute colitis based on 16S rRNA gene sequencing. *Chin Med J*. 2019;132(15):1833–1842. doi:10.1097/CM9.0000000000000308
34. Taddese R, Garza DR, Ruiter LN, et al. Growth rate alterations of human colorectal cancer cells by 157 gut bacteria. *Gut Microbes*. 2020;12 (1):1–20. doi:10.1080/19490976.2020.1799733
35. Luo J, Li T, Xie J, et al. Guar gum different from Ganoderma lucidum polysaccharide in alleviating colorectal cancer based on omics analysis. *Food Funct*. 2020;11(1):572–584. doi:10.1039/c9fo02786f
36. Brown EM, Ke X, Hitchcock D, et al. Bacteroides-derived sphingolipids are critical for maintaining intestinal homeostasis and symbiosis. *Cell Host Microbe*. 2019;25(5):668–680 e7. doi:10.1016/j.chom.2019.04.002
37. Yu B, Wang M, Teng B, et al. Partially acid-hydrolyzed porphyran improved dextran sulfate sodium-induced acute colitis by modulation of gut microbiota and enhancing the mucosal barrier. *J Agric Food Chem*. 2023;71(19):7299–7311. doi:10.1021/acs.jafc.2c08564
38. Wang C, Xiao Y, Yu L, et al. Protective effects of different Bacteroides vulgatus strains against lipopolysaccharide-induced acute intestinal injury, and their underlying functional genes. *J Adv Res*. 2022;36:27–37. doi:10.1016/j.jare.2021.06.012
39. Shalley S, Pradip Kumar S, Srinivas TN, Suresh K, Anil Kumar P. Marinilabilia nitratireducens sp. nov., a lipolytic bacterium of the family Marinilabiliaceae isolated from marine solar saltern. *Antonie Van Leeuwenhoek*. 2013;103(3):519–525. doi:10.1007/s10482-012-9834-8
40. Tian B, Zhao J, Zhang M, et al. Lycium ruthenicum anthocyanins attenuate high-fat diet-induced colonic barrier dysfunction and inflammation in mice by modulating the gut microbiota. *Mol Nutr Food Res*. 2021;65(8):e2000745. doi:10.1002/mnfr.202000745
41. Sheng L, Jena PK, Liu HX, et al. Gender differences in bile acids and microbiota in relationship with gender dissimilarity in steatosis induced by diet and FXR inactivation. *Sci Rep*. 2017;7(1):1748. doi:10.1038/s41598-017-01576-9
42. Niu X, Shang H, Chen S, et al. Effects of Pinus massoniana pollen polysaccharides on intestinal microenvironment and colitis in mice. *Food Funct*. 2021;12(1):252–266. doi:10.1039/d0fo02190c
43. Wang L, Liao Y, Yang R, et al. An engineered probiotic secreting Sj16 ameliorates colitis via Ruminococcaceae/butyrate/retinoic acid axis. *Bioeng Transl Med*. 2021;6(3):e10219. doi:10.1038/s41598-017-01576-9
44. Waters JL, Ley RE. The human gut bacteria Christensenellaceae are widespread, heritable, and associated with health. *BMC Biol*. 2019;17(1):83. doi:10.1002/btm2.10219